

Noise properties of high- T_c superconducting flux transformers fabricated using chemical-mechanical polishing

M. Chukharkin,^{1,2} A. Kalabukhov,^{1,2} J. F. Schneiderman,^{1,3} F. Öisjöen,¹ O. Snigirev,² Z. Lai,¹ and D. Winkler¹

¹Department of Microtechnology and Nanoscience—MC2, Chalmers University of Technology, Gothenburg, Sweden

²M.V. Lomonosov Moscow State University, Moscow, Russian Federation

³MedTech West, Sahlgrenska Academy and University of Gothenburg, Institute of Neuroscience and Physiology, Gothenburg, Sweden

(Received 25 May 2012; accepted 8 July 2012; published online 24 July 2012)

Reproducible high-temperature superconducting multilayer flux transformers were fabricated using chemical mechanical polishing. The measured magnetic field noise of the flip-chip magnetometer based on one such flux transformer with a $9 \times 9 \text{ mm}^2$ pickup loop coupled to a bicrystal dc SQUID was $15 \text{ fT/Hz}^{1/2}$ above 2 kHz. We present an investigation of excess $1/f$ noise observed at low frequencies and its relationship with the microstructure of the interlayer connections within the flux transformer. The developed high- T_c SQUID magnetometers may be advantageous in ultra-low field magnetic resonance imaging and, with improved low frequency noise, magnetoencephalography applications. © 2012 American Institute of Physics. [<http://dx.doi.org/10.1063/1.4738782>]

Magnetometers based on superconducting quantum interference devices (SQUIDs) are widely used in various biomedical applications, including magnetoencephalography (MEG)¹ and ultra-low field magnetic resonance imaging (ulf-MRI).² These applications demand magnetic field sensitivity of less than $10 \text{ fT/Hz}^{1/2}$; for MEG, the high sensitivity should also remain at frequencies as low as 10 Hz.^{3,4} This imposes strict requirements on the magnetic sensor performance. Low critical-temperature (low- T_c) SQUID magnetometers may yield magnetic field sensitivity below $1 \text{ fT/Hz}^{1/2}$, but they require liquid helium temperatures (4.2 K) for operation. To simplify cooling requirements, high critical-temperature (high- T_c) SQUIDs can be utilized that operate at the boiling point of liquid nitrogen (77 K). This may be advantageous, especially for MEG where the separation between the SQUID and scalp should be minimized. However, the magnetic field sensitivity of standard single-layer high- T_c SQUID magnetometers is typically a factor of 30 worse than equivalent low- T_c SQUIDs. A significant design limitation of such magnetometers is the very large inductance mismatch between the pick-up loop and the SQUID loop that reduces the effective area A_{eff} of the sensor (that equivalently increases the flux-to-field transformation coefficient A_{eff}^{-1} (nT/Φ_0), and thus the sensitivity of the sensor). A typical single-layer high- T_c dc SQUID magnetometer has a magnetic field sensitivity of $50 \text{ fT/Hz}^{1/2}$ at 10 Hz and transformation coefficient $A_{\text{eff}}^{-1} = 5.3 \text{ nT}/\Phi_0$.⁵ To improve the transformation coefficient and thus the magnetic field sensitivity of the sensors, flux transformers with a multiturn input coil should be used.

A superconducting flux transformer consists of a large superconducting pickup loop and a smaller multiturn input coil that couples magnetic flux into the SQUID (Ref. 6) (Figs. 1(a) and 1(b)). Flux transformers can either be integrated on the same chip with the SQUID or in a separate flip-chip configuration. The flip-chip configuration is easier to realize but requires accurate alignment between two chips in order to provide high mutual inductance.

Thin film flux transformers require two superconducting layers separated by an insulator. There should also be a superconducting connection (a via) between the superconducting layers. The main challenge for the fabrication of crossovers and vias in high- T_c superconducting materials is to obtain c-oriented film on the entire length of the top electrode. In order to provide proper conditions for the growth of c-oriented high- T_c film, very shallow edge slopes of the bottom electrode need to be produced. Another important issue is the smoothness of the bottom electrode because the presence of droplets and precipitates on its surface can lead to the formation of unwanted short-circuits between layers.

The early high- T_c thin film multilayer flux transformers were made with an ion-beam etching (IBE) technique.^{7–10} Slopes of $10\text{--}25^\circ$ were obtained using post exposure baking of the resist mask. Ludwig *et al.* fabricated a flip-chip SQUID magnetometer with a multilayer flux transformer with a magnetic field sensitivity of $74 \text{ fT/Hz}^{1/2}$ at 1 Hz and $31 \text{ fT/Hz}^{1/2}$ at 1 kHz.⁶ Drung *et al.* demonstrated sensitivity of an integrated multilayer SQUID magnetometer of $9.7 \text{ fT/Hz}^{1/2}$ at 1 kHz and $53 \text{ fT/Hz}^{1/2}$ at 1 Hz.¹⁰

The fabrication process was improved by using anisotropic chemical etching with a non-aqueous Br-ethanol solution.^{11–14} This technique yields slope edge angles down to 3° and was used to produce multilayer high- T_c superconductor flux transformers with a transformation coefficient of $1 \text{ nT}/\Phi_0$ on $10 \times 10 \text{ mm}^2$ chips.¹¹ The magnetic field sensitivity of magnetometers combined with such flux transformers was $15 \text{ fT/Hz}^{1/2}$ at 1 kHz and $35 \text{ fT/Hz}^{1/2}$ at 1 Hz for an $8 \times 8 \text{ mm}^2$ pickup loop and $3.5 \text{ fT/Hz}^{1/2}$ at 1 kHz and $7 \text{ fT/Hz}^{1/2}$ at 1 Hz for a $16 \times 16 \text{ mm}^2$ pickup loop.¹⁴

The chemical-mechanical polishing (CMP) method was suggested for fabrication of high- T_c multilayer structures as an alternative approach.^{15,16} CMP has several benefits when compared to previous techniques. CMP does not require hazardous chemicals like Br-ethanol. Polishing also improves surface smoothness of the bottom electrode, thereby reducing galvanic

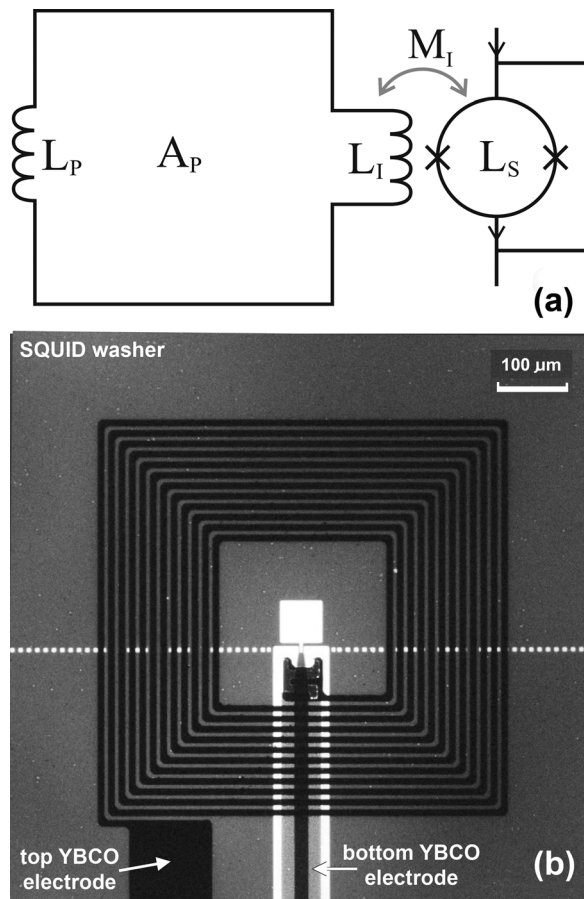


FIG. 1. (a) Schematic of the SQUID magnetometer with flux transformer. The optimal design maximizes the area of the pickup coil, A_P , while matching the pickup coil inductance, L_P , to that of the input coil, L_I , and making the coupling parameter, $\alpha = M_I/(L_I L_S)^{1/2}$, between the input coil and the SQUID as close to 1 as possible. (b) Image of our magnetic field flux transformer glued together with the SQUID.

shorts that plague methods that rely exclusively on chemical etching.^{17,18} It has further been shown that edge slope angles of less than 1° can be obtained using CMP, meaning crossovers with very high critical current densities (2×10^6 A/cm²) are within reach.¹⁵ Takashima *et al.* fabricated a CMP-based multilayer YBa₂Cu₃O_{7-x}/SrTiO₃/YBa₂Cu₃O_{7-x} (YBCO/STO/YBCO) SQUID magnetometer, but their device was limited to a single-turn input coil.¹⁹ CMP-processed multilayer high- T_c superconducting flux transformers with multiturn coils have yet to be experimentally realized.

In this work, we have implemented a safe and reproducible CMP process for fabrication of high- T_c superconducting multilayer flux transformers. Our YBCO/STO/PrBa₂Cu₃O₇/STO/YBCO crossovers and vias showed excellent superconducting parameters. The developed technique was used to fabricate multiturn magnetic flux transformers on 10×10 mm² STO substrates. A flip-chip design SQUID magnetometer combined with one such multilayer flux transformer demonstrated a magnetic field sensitivity of 15 fT/Hz^{1/2} at 2 kHz and 135 fT/Hz^{1/2} at 10 Hz. We present a study of the low frequency noise and its relationship with the microstructure of the interlayer connections in the flux transformer. High resolution transmission electron microscopy (HRTEM) investigations suggest the excess $1/f$ noise was caused by a-oriented grains in the top YBCO electrode. We

plan to use our developed high- T_c SQUID magnetometers in an ulf-MRI system and, with improved low frequency noise, for magnetoencephalography.

An image of the input coil of one of the flux transformers glued together with a SQUID is presented in Fig. 1(b). The interconnection line in the bottom electrode connected the middle part of the input coil to the outer pick-up loop. The SQUID had 1.5 μ m wide Josephson junctions and a washer size of 1.28×1.28 mm². Four identical SQUIDs were tested with this 10×10 mm² transformer chip.

The effective area of the magnetometer can be estimated using the formula,⁶

$$A_{eff} = \frac{\alpha}{2} A_P \frac{\sqrt{L_S}}{\sqrt{L_P}}, \quad (1)$$

where $0 < \alpha < 1$ is the coupling coefficient between the SQUID and the transformer input coil, A_P and L_P are the area and the inductance of the transformer pickup loop, respectively, and L_S is the SQUID inductance (see Fig. 1(a)). This expression shows that the effective area of a SQUID magnetometer with a flux transformer is increased by a factor of $\frac{1}{2} \frac{\sqrt{L_P}}{\sqrt{L_S}}$ as compared to a single-layer (directly coupled) magnetometer of equivalent size $A_{eff} = \alpha A_P \frac{L_S}{L_P}$ (i.e., the inductances, L_P , and effective areas, A_P , of the pick-up coils would be roughly the same in both cases).

The SQUID had a square 60×60 μ m² hole that corresponded to a calculated inductance of $L_S = 100$ pH. The flux transformer consisted of a square pick-up loop with the outer dimension $D = 9$ mm and the inner dimension $d = 8$ mm that corresponded to $A_P = D \times d$ of about 72 mm². The calculated inductance of the pick-up loop L_P was 20 nH.⁶ The multiturn input coil had 11 turns and 10 μ m line-widths with 5 μ m pitch, providing an inductance of about $L_I = 25$ nH.

The YBCO thin films were grown by pulsed laser deposition (heater temperature 810 $^\circ$ C, oxygen pressure 0.6 mbar, energy density of 1.46 J/cm²). The deposited thickness of both bottom and top YBCO layers was 360 nm. The insulating trilayer of STO/PBCO/STO was deposited using RF sputtering. The two 30 nm thick layers of SrTiO₃ were deposited with an RF source power of 100 W in a mixed argon-oxygen atmosphere (60% O₂ + 40% Ar) at a partial pressure of 0.1 mbar. A 300 nm PBCO layer was deposited in between the STO layers under the same partial pressure of gas with a mixture of 20% O₂ + 80% Ar and an RF source power of 50 W.

A Logitech PM5 polishing machine was used to polish the YBCO films and the insulating trilayer. The polishing fluid (Logitech SF1) consisted of formaldehyde (<1.0%), ethylene glycol (4%-5%), and amorphous silica (15%-50%). The size of the amorphous silica particles was 20–140 nm. The polishing platen covered with a soft polyurethane pad rotated at constant speed that could be selected between 1 and 70 rpm. Samples were mounted on the glass holder that performed rotational movements on the platen surface. It was possible to attach weight to the glass holder in the range of 400–1500 g. Several dummy STO substrates were mounted on the holder to improve uniformity of the weight distribution.

The polished surface of the YBCO films was very smooth, with roughness r_a (arithmetic average of absolute

values) below 1 nm. Scanning electron microscopy (SEM) and energy-dispersive x-ray spectroscopy (EDS) investigations did not show any foreign contaminations of the film surface after polishing. Furthermore, measurements of the critical temperature of the bottom YBCO film indicated that there was no degradation of its superconducting properties after the polishing procedure.

The fabrication process for the YBCO/(STO/PBCO/STO)/YBCO multilayer structures using the optimized CMP process is described below. The bottom YBCO film was patterned using ultraviolet (UV) photolithography and dry Ar^+ IBE. After the etching, the measured slope angle of edges in the YBCO film was around 60° . The polishing procedure was applied to reduce the angle of the slope edge to about 2° . After this, deposition of the insulating layer and patterning of the windows for vias was performed. A second polishing step was used to obtain shallow slope angles in the insulator. Finally, deposition of the top YBCO film and patterning of the top electrode were performed using UV photolithography and IBE.

Several test crossovers and vias were made to examine the fabrication process. The critical temperatures of the bottom and top electrodes were typically 89–90 K. The critical current densities of both electrodes including crossover parts were $6 \times 10^6 \text{ A/cm}^2$. These high critical parameters indicate that the fabrication process did not degrade the superconducting properties of the films.

The measured critical current of the vias was about 80 mA. This is sufficiently higher than the currents that would be induced by typical signals in MEG and ulf-MRI. It is difficult to estimate the critical current density in the vias due to the anisotropy of the superconducting properties of the YBCO. Since the critical current density of YBCO in the a-b planes is about 100 times higher than that along the c-axis direction, the cross-sectional area of the via that dominates supercurrent transport is mainly defined by the perimeter of the window and overlap between the top and bottom electrodes on the slopes of the edges.

The flux transformers were fabricated with our CMP process on double-side polished $10 \times 10 \text{ mm}^2$ STO substrates. In order to improve the reproducibility of the process, the interconnection line was fabricated in the bottom electrode followed by fabrication of the input coil in the top electrode. The top electrode thus contains both the pick-up loop and the multi-turn input coil. This process had a high fabrication yield of 90% (11 out of 12 samples).

The SQUIDs were fabricated on separate $10 \times 10 \text{ mm}^2$ 24° bicrystal substrates. The flux transformers and SQUID chips were glued together using UV5 photoresist. Chips were dried for 2 h at room temperature after alignment. The in-plane misalignment between chips was estimated to be less than $2 \mu\text{m}$ (see Fig. 1(b)).

Measurements of the SQUID magnetometer transformation coefficient A_{eff}^{-1} were performed using a calibrated Helmholtz coil set with an outer diameter of 40 cm. MAGNICON SEL-1 electronics was used for control and readout of the SQUID. Noise measurements were recorded with a Stanford Research 785 spectrum analyzer. For magnetic flux noise measurements, a 4-layer permalloy shield was used in addition to a superconducting shield. In order to reduce the

contribution of critical current fluctuations in the junctions of the bicrystal SQUID, the device was operated with a bias reversal technique at 40 kHz.²⁰

The measured transformation coefficient of one of the flip-chip SQUID + transformer magnetometers was $A_{\text{eff}}^{-1} = 1.6 \text{ nT}/\Phi_0$. This value corresponds to an estimated coupling coefficient of $\alpha = 0.51$ (Eq. (1)). In order to better understand the coupling mechanism between the SQUID washer and the input coil, we made calculations of this mutual inductance with 3D-MLSI software.²¹ The calculations were made using the designed chip layout and assuming the distance between the SQUID and the flux transformer chip was $3 \mu\text{m}$ (mechanical micrometer measurements of this distance indicate it lies between 1 and $5 \mu\text{m}$). The calculated coupling coefficient was $\alpha = 0.41$. The resulting agreement between calculated and estimated coupling coefficients ($\alpha = 0.41$ and $\alpha = 0.51$, respectively) indicates the alignment between the SQUID and transformer chips was near optimal. The better value of measured coupling coefficient can be explained that the distance between was likely less than $3 \mu\text{m}$ in the experiment.

Noise spectra of the flip-chip magnetometer and bare SQUID in ac-bias mode are shown in Fig. 2. The bare SQUID (i.e., without the transformer) had a magnetic flux noise of about $10 \mu\Phi_0/\text{Hz}^{1/2}$ with a $1/f$ cut-off frequency of about 10 Hz in ac-bias mode. When the SQUID was coupled to the flux transformer, the white noise level above 2 kHz remained the same and corresponded to a magnetic field sensitivity of about $15 \text{ fT}/\text{Hz}^{1/2}$. Below 2 kHz, however, excess $1/f$ noise was observed that was not suppressed by ac-bias. We attribute this excess noise to the presence of the flux transformer.

A possible source of low-frequency noise in the flux transformer is thermally activated motion of flux vortices trapped in the high- T_c film.⁶ We performed several experiments in order to investigate the possible microscopic origin of the excess noise. We measured the noise properties of the

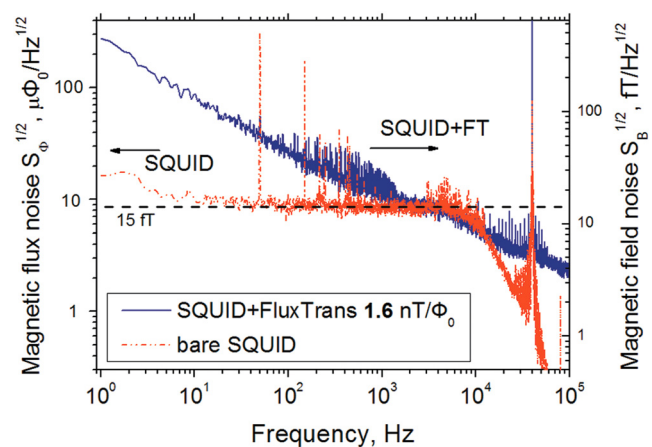


FIG. 2. Noise spectra of the bicrystal dc SQUID (dashed) and the same SQUID coupled with our multiturn superconducting flux transformer fabricated using CMP (solid). The left axis indicates the flux noise for both the bare SQUID and the SQUID coupled with flux transformer. The right axis is the calibrated magnetic field noise spectra of the SQUID and flux transformer. Note the white noise level of $15 \text{ fT}/\text{Hz}^{1/2}$ above 1 kHz obtained with the optimized device. The excess $1/f$ noise contributed by the flux transformer is likely caused by flux motion in grain boundaries within the vias (see text).

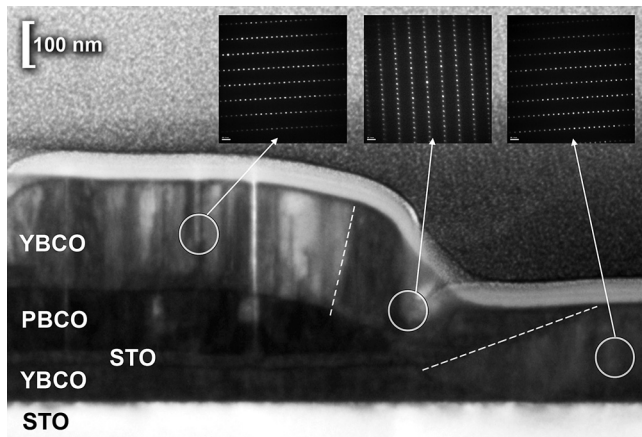


FIG. 3. Cross-sectional high resolution transmission electron microscope image of interlayer connection (via) of the flux transformer presented herein. Insets show SAED images from three different locations in the top $\text{YBa}_2\text{Cu}_3\text{O}_{7-x}$ electrode. Dashed lines indicate the boundaries between a-axis and c-axis oriented grains of the YBCO film. Note the high quality interface between top and bottom YBCO electrodes.

flux transformer after etching a cut in the input coil, thereby decoupling it from the pickup loop. The measured flux noise in that case showed the same excess $1/f$ noise. This indicates that currents circulating around the pickup loop did not contribute significantly to the flux noise. We therefore assumed that the source of the flux noise is located in the multilayer structures. We then attempted to determine what part of the multilayer structures (crossovers or vias) were the main culprits. We fabricated a flux transformer with a square interconnection line that was wider than the input coil of the transformer. In this case, only two wide crossovers in the pickup loop are needed. The central via was thus the only multilayer sub-structure that remained close to the SQUID washer. The noise measurements of such a flux transformer showed essentially the same noise behavior. We therefore concluded that the source of the excess $1/f$ noise is most probably to be found in the interconnections (vias) between the superconducting electrodes. We have not, however, eliminated the possibility that some noise also originates from flux motion in the top YBCO electrode.

We investigated the microstructure of the vias using high resolution transmission electron microscopy (HR-TEM), see Fig. 3. These measurements revealed the high quality nature of the interfaces between the top and bottom YBCO layers. Our CMP method is thus a promising technique for fabrication of multilayer structures in high- T_c materials.

Selected area electron diffraction (SAED) investigations (see insets in Fig. 3) of the top electrode showed that the top YBCO film had grains with a-orientation on the slope of the via. The rest of the top electrode had c-orientation. The dashed lines in Fig. 3 indicate the boundaries between regions of different orientation. The bottom STO layer in the insulator stack could be a possible source of nucleation for a-oriented YBCO growth. The a-oriented YBCO grains are known to enhance the motion of flux vortices²² and can therefore be a possible source for increased magnetic flux noise in our flux transformers. Removing the bottom STO layer from the insulator stack may reduce the number of

a-oriented grains from the top YBCO film on the via and thus improve the noise properties of our flip-chip SQUID magnetometers.

In conclusion, the CMP method was implemented for fabrication of high- T_c multilayer superconducting flux transformers. The advantage of using polishing is the capability to reduce edge slope angles to just a few degrees without the need for toxic chemicals. Furthermore, the process yields surface-smoothness that reduces the prevalence of interlayer short circuits, thereby increasing yield. Combined with bicrystal high- T_c SQUID sensors, these transformers enable at least a 3-fold gain in sensitivity when compared to standard single-layer high- T_c SQUID sensors of the same size. The measured magnetic field sensitivity of the flip-chip SQUID magnetometer fabricated using developed CMP polishing was $15 \text{ fT/Hz}^{1/2}$ at 2 kHz and $135 \text{ fT/Hz}^{1/2}$ at 10 Hz. Due to the high sensitivity, our flip-chip SQUID magnetometers are promising sensors with improved low frequency noise for MEG. Furthermore, we are presently developing an ultra-low field MRI system that includes a copper flux transformer and high- T_c SQUID sensor technology similar to that developed, for example, by Chen *et al.*²³ The advanced magnetometers developed herein are a promising technology for improving the sensitivity of this ultra-low field MRI system operating in the kHz frequency range.

Fruitful discussions with J. Clarke are acknowledged. The work is supported by European FP7 project “MEGMRI,” contract number 200859, The Swedish Research Council, Knut and Alice Wallenberg foundation, the European Union via Tillväxtverket and Regionala Utvecklingsfonden for MedTech West, and Kristina Stenborgs stiftelse. One of the authors (O.S.) appreciates support from RFBR Grant #11-02-01238-a.

- ¹C. Del Gratta, V. Pizzella, F. Tecchio, and G. L. Romani, *Rep. Prog. Phys.* **64**, 1759 (2001).
- ²J. Clarke, M. Hatridge, and M. Mössle, *Annu. Rev. Biomed. Eng.* **9**, 389 (2007).
- ³M. Burghoff, H. H. Albrecht, S. Hartwig, I. Hilschenz, R. Korber, T. S. Thommes, H. J. Scheer, J. Voigt, and L. Trahms, *Metrolog. Meas. Syst.* **16**, 371 (2009).
- ⁴A. I. Ahonen, M. S. Hamalainen, M. J. Kajola, J. E. T. Knuutila, P. P. Laine, O. V. Lounasmaa, L. T. Parkkonen, J. T. Simola, and C. D. Tesche, *Phys. Scr.* **T49a**, 198 (1993).
- ⁵F. Öisjöen, J. F. Schneiderman, G. A. Figueras, M. L. Chukharkin, A. Kalabukhov, A. Hedström, M. Elam, and D. Winkler, *Appl. Phys. Lett.* **100**, 132601 (2012).
- ⁶F. Ludwig, E. Dantsker, D. Koelle, R. Kleiner, A. H. Miklich, and J. Clarke, *Appl. Supercond.* **3**, 383 (1995).
- ⁷D. Grundler, B. David, R. Eckart, and O. Dössel, *Appl. Phys. Lett.* **63**, 2700 (1993).
- ⁸F. Ludwig, D. Koelle, E. Dantsker, D. T. Nemeth, A. H. Miklich, and J. Clarke, *Appl. Phys. Lett.* **66**, 373 (1995).
- ⁹M. N. Keene, S. W. Goodyear, N. G. Chew, R. G. Humphreys, J. S. Satchell, J. A. Edwards, and K. Lander, *Appl. Phys. Lett.* **64**, 366 (1994).
- ¹⁰D. Drung, F. Ludwig, W. Müller, U. Steinhoff, L. Trahms, H. Koch, Y. Q. Shen, M. B. Jensen, P. Vase, T. Holst *et al.*, *Appl. Phys. Lett.* **68**, 1421 (1996).
- ¹¹M. I. Faley, U. Poppe, K. Urban, D. N. Paulson, T. N. Starr, and R. L. Fagaly, *IEEE Trans. Appl. Supercond.* **11**, 1383 (2001).
- ¹²M. I. Faley, U. Poppe, H. Soltner, C. L. Jia, M. Siegel, and K. Urban, *Appl. Phys. Lett.* **63**, 2138 (1993).
- ¹³C. L. Jia, M. I. Faley, U. Poppe, and K. Urban, *Appl. Phys. Lett.* **67**, 3635 (1995).
- ¹⁴M. I. Faley, U. Poppe, K. Urban, D. N. Paulson, and R. L. Fagaly, *J. Phys., Conf. Ser.* **43**, 1199 (2006).

- ¹⁵H. Takashima, N. Terada, and M. Koyanagi, *IEEE Trans. Appl. Supercond.* **9**, 3464 (1999).
- ¹⁶H. Takashima, N. Kasai, and A. Shoji, *Jpn. J. Appl. Phys.* **41**, L1062 (2002).
- ¹⁷Y. Wada, K. Kuroda, and T. Takami, *IEEE Trans. Appl. Supercond.* **13**, 817 (2003).
- ¹⁸K. Kuroda, Y. Wada, T. Takami, and T. Ozeki, *Jpn. J. Appl. Phys.* **42**, L1006 (2003).
- ¹⁹H. Takashima, N. Kasai, and A. Shoji, *Physica C* **392**, 1367 (2003).
- ²⁰D. Drung, *Supercond. Sci. Technol.* **16**, 1320 (2003).
- ²¹M. M. Khapaev, M. Yu. Kupriyanov, E. Goldobin, and M. Siegel, *Supercond. Sci. Technol.* **16**, 24 (2003).
- ²²M. J. Ferrari, M. Johnson, F. C. Wellstood, J. J. Kingston, T. J. Shaw, and J. Clarke, *J. Low Temp. Phys.* **94**, 15 (1994).
- ²³H. Chen, H. Yang, H. Horng, S. Liao, S. Yueh Yang, and L. Wang, *J. Appl. Phys.* **110**, 093903 (2011).